2023 62nd IEEE Conference on Decision and Control (CDC)
December 13-15, 2023. Marina Bay Sands, Singapore

State estimation for enhanced low dimensional electrochemical models of lithium-ion batteries

Mira Khalil[1,2], Romain Postoyan[1] and Stéphane Raël[2]

***Abstract*— Safe and efficient operation of lithium-ion batteries requires an accurate estimation of the internal states. One approach is to design an observer based on an electrochemical model of the battery internal dynamics. However, electrochemical models, and their associated observers, typically require a high dimension to generate accurate variables. In this paper, we explain how to alleviate this limitation by correcting the lithium concentrations generated by a finite-dimensional electrochemical model derived from the spatial discretizations of partial differential equations (PDE). We show that the corrected concentrations asymptotically match those generated by the original PDEs for constant input currents, irrespectively of the order of the considered finite-dimensional model. We then exploit this fact to derive a new state space model for which we design an observer, whose global, robust convergence is supported by a Lyapunov analysis provided a linear matrix inequality holds. The estimated concentrations are then corrected to asymptotically match those of the original PDEs in absence of disturbances for constant currents. Simulation results show improvements both in terms of modeling and estimation accuracy as a result of the proposed corrections.**

I. Introduction

Lithium-ion batteries present many advantages in terms of volume capacity, weight, power density, as well as the absence of memory effect. Nevertheless, this type of batteries require a battery management system (BMS) to make them safe, reliable and efficient. The BMS needs to be fed with accurate information on the state of the battery for this purpose. Unfortunately, some key battery variables cannot be measured directly with sensors, which means that they have to be estimated.

A popular method to estimate the internal state of a lithium-ion battery consists in designing an observer based on a mathematical model of the battery internal dynamics. Several types of battery models are available in the literature for this purpose, see e.g., [11], [15]. The simplest ones consist in representing the battery dynamics by an equivalent circuit model made of few resistors and capacitors, see e.g., [1], [2]. This apparent simplicity has a price nevertheless: the model requires a non-trivial parameterization to provide accurate data in general, see e.g., [14]. An alternative is based on electrochemical models, which locally describe the physics of lithium-ion cell operation using partial differential equations (PDE), see e.g., [8], [10]. Electrochemical models often rely on the assumption that the particles within an electrode behave like an average particle, we talk of single particle models (SPM) as in e.g., [4]–[7], [16], [17]. The corresponding infinite-dimensional model can then be spatially discretized to obtain a finite-dimensional model, which is convenient to design and implement a state observer. Finite-dimensional models typically require a high dimension to generate accurate battery variables, as the latter are affected by the errors resulting from the spatial discretization of the original PDEs. This may be problematic as the derived observer may then be of high dimension, which may make its design numerically challenging and may be an obstacle for its implementation.

In this work, we present a method to alleviate the need for finite-dimensional models of high dimension to generate accurate variables. We consider for this purpose the finite-dimensional model of [5], whose dimension is directly related to the number of samples of the PDEs and can therefore be freely selected. We then present a technique to systematically correct the concentrations generated by this model so that these asymptotically match the concentrations given by the original PDEs for constant currents. Hence, for any given model order, the corrected concentrations from the finite-dimensional model asymptotically tend to the actual concentrations of the original infinite-dimensional model for constant inputs thereby asymptotically eliminating the errors induced by spatial discretization. Although the purpose of these corrections is to eliminate asymptotic errors for constant inputs, the provided simulation results show that significant improvements are also obtained for short time horizons with a rapidly changing current profile. We then exploit these corrected concentrations to derive a new output voltage equation, which leads to a new state space model.

Afterwards, we design an observer for this new model. We present a method for this purpose based on polytopic and Lyapunov-based tools similarly to e.g., [4], [9], [19]. This method guarantees the robust convergence of the state estimates generated by the observer to the actual battery states provided a linear matrix inequality holds. We then explain how to correct the estimated concentrations to asymptotically track those of the original PDEs in absence of disturbances and for constant inputs. Simulation results are presented to illustrate the improvements brought by the corrected model and the associated estimation scheme. The definitions and numerical values of all the parameters, as well as all the proofs are given in the extended version of this work in [12].

Notation. Let $\mathbb{R}$ be the set of real numbers, $\mathbb{R}_{>0} := (0,\infty)$, $\mathbb{R}_{\geq 0} := [0,\infty)$, $\mathbb{R}_{<0} := (-\infty,0)$, $\mathbb{Z}$ be the set of integers, $\mathbb{Z}_{>0} := \{1,2,3,...\}$. We use $\mathbb{I}_n$ to denote the identity matrix

*This work was funded by Lorraine Université d'Excellence LUE.

[1]Université de Lorraine, CNRS, CRAN, F-54000 Nancy, France. (mira.khalil@univ-lorraine.fr, romain.postoyan@univ-lorraine.fr).

[2]Université de Lorraine, GREEN, F-54000 Nancy, France. (stephane.rael@univ-lorraine.fr).

of dimension n and $\mathbf{1}_{n\times m}$ the matrix of $\mathbb{R}^{n\times m}$ whose elements are all equal to 1, with $n,m\in\mathbb{Z}_{>0}$. Given square matrices $A_1,...,A_n$, $\mathrm{diag}(A_1,...,A_n)$ is the block diagonal matrix, whose block diagonal components are $A_1,...,A_n$ and $\underline{\mathrm{diag}}(A_1,...,A_n)$ ($\overline{\mathrm{diag}}(A_1,...,A_n)$) is the lower (upper) block diagonal matrix, whose lower (upper) block diagonal components are $A_1,...,A_n$. Given a vector $x\in\mathbb{R}^n$, $x^\top$ denotes the transpose of x. Given $x\in\mathbb{R}^n$ and $y\in\mathbb{R}^m$ with $n,m\in\mathbb{Z}_{>0}$, we use the notation (x,y) to denote $(x^\top,y^\top)^\top$. Given $f:\mathbb{R}\to\mathbb{R}^n$ with $n\in\mathbb{Z}_{>0}$, $(f)_\infty$ stands for $\lim_{t\to\infty}f(t)$ when it exists. For a vector $x\in\mathbb{R}^N$, $|x|$ denotes its Euclidean norm. For a matrix $A\in\mathbb{R}^{n\times m}$, $\|A\|$ stands for its 2-induced norm and for any $i\in\mathbb{R}^n$, $j\in\mathbb{R}^m$, $(A)_{ij}$ represents the j-th element of the i-th row of matrix A. Let $f:\mathbb{R}_{\geq 0}\to\mathbb{R}^N$, $\|f\|_{\mathscr{L}_2,[0,t)}$ denotes the $\mathscr{L}_2$ norm of f on the interval $[0,t)$, where $t\in[0,\infty]$. We write $f\in\mathscr{L}_2$, when $\|f\|_{\mathscr{L}_2,[0,\infty)}<\infty$.

II. Battery model

We recall the SPM model in [5], and we explain how to correct its lithium concentrations. Those concentrations are then exploited to derive a new output equation and the new model is finally given in a state space form.

A. Preliminaries on the model in [5]

We first briefly recall the main elements of a lithium-ion cell, namely: the positive electrode, the separator and the negative electrode, which are all immersed in the electrolyte, and two current collectors. The electrolyte is an ionic solution that ensures ion transport within the battery. The porous separator is an electrical insulator that does not allow electrons to flow between the two electrodes. However, being porous, it allows the passage of ions via the electrolyte. The positive and negative electrodes consist of almost spherical particles of porous materials. The electrodes structure creates a surface of contact between the electrodes and the electrolyte producing electrochemical couples between them and thus introducing a potential difference between the positive and negative electrode.

The considered electrochemical model relies on the next assumption.

Standing Assumption 1 (SA1): The following holds: (i) lithium insertion or de-insertion reactions are homogeneous along the thickness of each electrode; (ii) the electrolyte dynamics is neglected; (iii) the temperature of the cell is constant and homogeneous. □

Item (i) implies that each electrode can be reduced to a single particle, whose size is equal to the average size of all the particles that compose the actual electrode, we talk of SPM assumption, see e.g., [4]–[7], [16], [17]. As customarily done in electrochemical modeling of lithium-ion batteries, electrodes material particles are supposed spherical. In item (ii), we ignore the electrolyte dynamics, which is reasonable for moderate currents and moderate temperatures. For high current rates and/or low temperatures, item (ii) can be relaxed and electrolyte dynamics can be added to the presented model and observer by applying the results of [3]. In item (iii), we suppose that the temperature is constant however, when the temperature varies, and is measured we can adapt the model and the developed observer of Section III.A to take into account the temperature variation like in [4], [17]. As for the temperature homogeneity assumption, it is reasonable at moderate and high temperatures. For low temperatures, it may become invalid and be interpreted as a parametric uncertainty, which can be handled by the observer of Section III.A if the uncertainty is small enough, see [17].

Given SA1, the main dynamical phenomenon is the lithium diffusion in the electrodes active particles. This phenomenon is described using the next PDEs (see [8]), for any $t\geq 0$ and $r\in[0,R_s]$, where $R_s>0$ is the radius of the particle in electrode $s\in\{\mathrm{neg},\mathrm{pos}\}$, with neg and pos denoting the negative and positive electrode, respectively,

$$\begin{array}{rcl}\varphi_s(r,t) & = & -D_s\frac{\partial c_s(r,t)}{\partial r}\\ \frac{\partial c_s(r,t)}{\partial t} & = & \frac{1}{r^2}\frac{\partial}{\partial r}\left(D_s r^2\frac{\partial c_s(r,t)}{\partial r}\right),\end{array}\qquad(1)$$

where c_s is the local concentration of lithium, φ_s is the lithium flux density and $D_s>0$ is the diffusion coefficient of lithium, along with two boundary conditions $\varphi_s(0,t)=0$ and $\varphi_s(R_s,t)=\frac{j_s^{\mathrm{Li}}}{a_sF}$, where $j_s^{\mathrm{Li}}\in\mathbb{R}$ is the electrochemical reaction rate, $a_s:=\frac{3\varepsilon_s}{R_s}$ is the active surface per volume unit, $\varepsilon_s>0$ is the volume fraction of the active material particle and $F>0$ is Faraday's constant.

To derive a set of ordinary differential equations (ODE) from (1), a spatial discretization with uniform volume is performed. In particular, each particle is discretized into $N_s\in\mathbb{Z}_{>0}$ samples each having the same volume, where $s\in\{\mathrm{neg},\mathrm{pos}\}$. A zero-order approximation is made, i.e., we assume that the lithium concentration in each sample, $c_{s,n}$ for $n\in\{1,...,N_s\}$ and $s\in\{\mathrm{neg},\mathrm{pos}\}$, is homogeneous. From the obtained set of ODEs, we derive the next state space equation, with the index $s\in\{\mathrm{neg},\mathrm{pos}\}$

$$\dot{x}_s=A_sx_s+B_sm_s,\qquad(2)$$

where $x_s:=(c_{s,1},\ldots,c_{s,N_s})\in\mathbb{R}^{N_s}$ is the concatenation of the concentrations in electrode s and $m_s:=-\frac{j_s^{\mathrm{Li}}}{\varepsilon_sF}\in\mathbb{R}$ is the input. The matrices $A_s\in\mathbb{R}^{N_s\times N_s}$ and $B_s\in\mathbb{R}^{N_s\times 1}$ are defined as $A_s:=\mathrm{diag}(-\mu_1^s,-\upsilon_2^s,\ldots,-\upsilon_{N_s-1}^s,-\tilde{\mu}_{N_s}^s)+\underline{\mathrm{diag}}(\tilde{\mu}_2^s,\ldots,\tilde{\mu}_{N_s}^s)+\overline{\mathrm{diag}}(\mu_1^s,\ldots,\mu_{N_s-1}^s)$, $B_s:=\begin{pmatrix}0&\ldots&0&N_s\end{pmatrix}^\top$, where $\mu_i^s:=\frac{S_i^s}{r_{i+1}^s-r_i^s}\frac{D_s}{V_s}$ for any $i\in\{1,\ldots,N_s-1\}$, $\tilde{\mu}_i^s:=\frac{S_{i-1}^s}{r_i^s-r_{i-1}^s}\frac{D_s}{V_s}$ for any $i\in\{2,\ldots,N_s\}$, $\upsilon_i^s:=\tilde{\mu}_i^s+\mu_i^s$ for any $i\in\{2,\ldots,N_s-1\}$, $V_s:=\frac{1}{N_s}\frac{4}{3}\pi R_s^3$, $r_i^s:=\left(\frac{i}{N_s}\right)^{1/3}R_s$ and $S_i^s:=4\pi(r_i^s)^2$.

B. Concentrations correction

The spatial discretization of (1) to obtain (2) generates errors on the concentrations given by (2). These errors can be reduced by increasing the number of samples N_s, $s\in\{\mathrm{neg},\mathrm{pos}\}$, but this leads to a high-dimensional system in (2), which may lead to computational issues, especially when using the model in (2) for observer design. We present in this section an alternative method to reduce these errors by correcting the lithium concentrations generated by (2)

so that they asymptotically match those given by (1) for constant inputs, as formalized in the sequel. We can already emphasize that, although these corrections are established by considering the asymptotic behavior of (1) and (2) for constant inputs, these allow improving the accuracy of the concentrations given by (2) even for rapidly changing inputs as illustrated in Section IV. In this section, we denote by $c_{s,(1)}$ the lithium concentrations generated from the PDEs in (1) and $c_{s,(2)} := x_s$ the lithium concentrations generated by model (2) for electrode s, with $s \in \{\text{neg}, \text{pos}\}$.

We denote the corrected lithium concentrations of model (2) as $c_{s,\text{cor}}$, which are defined by, for $j \in \{1, \dots, N_s\}$ and $s \in \{\text{neg}, \text{pos}\}$,

$$c_{s,\text{cor},j} := c_{s,\text{mean}} - K_j^s (c_{s,\text{mean}} - c_{s,(2),j}), \tag{3}$$

where $c_{s,\text{mean}} := \frac{1}{N_s} \sum_{n=1}^{N_s} c_{s,(2),n}$ is the lithium-ion mean concentration in electrode s given by model (2) and $K_j^s \in \mathbb{R}$ is a static correction coefficient given in [12, (4)].

We present the next result on the error between the corrected concentrations of model (2) and the original concentrations of the PDEs in (1) when time tends to infinity for constant inputs.

Theorem 1: For a constant input m_s and an initial uniform profile for $c_{s,(1)}$, in the sense that there exists $c_0 \in \mathbb{R}_{\geq 0}$ such that for any $r \in [0, R_s]$ $c_{s,(1)}(r,0) = c_0$, any corresponding solution $c_{s,(1)}$ to (1) and $c_{s,(2)}$ to (2) with $c_{s,(2)}(0) = \mathbf{1}_{N_s \times 1} c_0$ satisfy for any $j \in \{1, \dots, N_s\}$ and $s \in \{\text{neg}, \text{pos}\}$

$$(c_{s,\text{cor},j} - c_{s,(1)}(r_j^s, \cdot))_\infty = 0, \tag{4}$$

where $c_{s,\text{cor}}$ is defined in (3). □

Theorem 1 implies that, as times tends to infinity, the corrected concentrations defined in (3) match those generated by the PDEs in (1) when the input is constant and $c_{s,(1)}(\cdot, 0)$ is uniform. It is important to note that Theorem 1 imposes no conditions on the number of samples with which the PDEs in (1) are discretized, and thus no conditions on the dimension of (2) for (4) to hold.

Remark 1: In Theorem 1, the lithium concentrations $c_{s,(1)}$ have an initial uniform profile. We claim that this is not restrictive as there are always periods of time in the life of a lithium-ion battery where $c_{s,(1)}$ is homogeneous in electrode s, with $s \in \{\text{neg}, \text{pos}\}$. □

C. Towards a state space model

Before we present the new output equation derived from (3), we recall the relation between m_s in (2) and the cell current I_{cell} and we perform a model reduction, which is essential to ensure the system detectability. Given SA1, the electrochemical reaction rate is homogeneous within each electrode. Therefore, a proportional relationship can be established between I_{cell} and j_s^{Li} in particular $j_{\text{neg}}^{\text{Li}} := \frac{I_{\text{cell}}}{A_{\text{cell}} d_{\text{neg}}}$ and $j_{\text{pos}}^{\text{Li}} := -\frac{I_{\text{cell}}}{A_{\text{cell}} d_{\text{pos}}}$, where I_{cell} is in generator convention (i.e., $I_{\text{cell}} > 0$ in discharge), A_{cell} is the electrode surface and d_s is the thickness of electrode s. On the other hand, we have $m_s := -\frac{j_s^{\text{Li}}}{\varepsilon_s F}$. Hence, we obtain $m_{\text{neg}} := -\frac{I_{\text{cell}}}{\varepsilon_{\text{neg}} A_{\text{cell}} d_{\text{neg}} F}$ and $m_{\text{pos}} := \frac{I_{\text{cell}}}{\varepsilon_{\text{pos}} A_{\text{cell}} d_{\text{pos}} F}$.

On the other hand, model (2) is reduced just like in e.g., [5], [13], [17] by adopting the next assumption, which is essential later for the observer convergence.

Standing Assumption 2 (SA2): The quantity of lithium inserted in battery electrodes is constant and known. □

SA2 is reasonable over short periods of time. Factors such as cell degradation or side reactions can cause capacity loss over time, resulting in a reduction in the total quantity of lithium and the violation of SA2. In this case, if there is a small uncertainty regarding the quantity of lithium, the battery state and its estimation would exhibit asymptotic small errors. Conversely, if the uncertainty is big and thus the quantity of lithium needs to be estimated, state of health estimation algorithms may be employed. SA2 allows to write a lithium mass conservation. Hence, the quantity of lithium is defined as

$$Q := \alpha_{\text{neg}} \sum_{i=1}^{N_{\text{neg}}} c_{\text{neg},i} V_{\text{neg}} + \alpha_{\text{pos}} \sum_{i=1}^{N_{\text{pos}}} c_{\text{pos},i} V_{\text{pos}}, \tag{5}$$

and is constant over time, where $\alpha_s := \frac{F}{3600} \frac{\varepsilon_s A_{\text{cell}} d_s}{V_s^{\text{total}}}$ and $V_s^{\text{total}} := N_s V_s$ is the volume of the particle of electrode s. From (5), we express the lithium concentration at the center of the negative electrode $c_{\text{neg},1}$ as a linear combination of all the other sampled concentration in solid phase

$$c_{\text{neg},1} = \overline{K} - \sum_{i=2}^{N_{\text{neg}}} c_{\text{neg},i} - \frac{\alpha_{\text{pos}} V_{\text{pos}}}{\alpha_{\text{neg}} V_{\text{neg}}} \sum_{i=1}^{N_{\text{pos}}} c_{\text{pos},i}, \tag{6}$$

where $\overline{K} := \frac{Q}{\alpha_{\text{neg}} V_{\text{neg}}}$.

In view of (6), $c_{\text{neg},1}$ is no longer needed in the state space representation as it can be recovered from the other concentrations.

D. Corrected output equation

We are ready to present the new output voltage equation. The output equation of model (2) is obtained by decomposition of the cell voltage V_{cell}. The main components of V_{cell} are the potential differences between the electrodes and the electrolyte called open circuit voltages (OCV) denoted OCV_s for $s \in \{\text{neg}, \text{pos}\}$, which depend on the surface insertion rates ζ_s defined by $\zeta_s := \frac{c_{s,N_s}}{c_{\max}^s}$ for $s \in \{\text{neg}, \text{pos}\}$, where $c_{\max}^s$ is the maximum lithium concentration of electrode s and c_{s,N_s} is the surface concentration generated by model (2). Given the lithium concentrations correction made in Section II.B, instead of using c_{s,N_s} to define the surface insertion rates, we use the corrected surface concentration c_{s,cor,N_s} defined in (3) to derive the corrected surface insertion rates $\zeta_{s,\text{cor}}$. As a result, we obtain the output equation for $y := V_{\text{cell}}$

$$y = OCV_{\text{pos}}(\zeta_{\text{pos,cor}}) - OCV_{\text{neg}}(\zeta_{\text{neg,cor}}) + g(u), \tag{7}$$

where $\zeta_{s,\text{cor}} := \frac{c_{s,\text{cor},N_s}}{c_{\max}^s}$ and $g(u) := -\eta_{r,\text{pos}}(u) - \eta_{\text{pos}}(u) - \eta_{\text{neg}}(u) - \eta_{r,\text{neg}}(u) - \eta_{r,\text{sep}}(u)$ for any $u := I_{\text{cell}} \in \mathbb{R}$, where $\eta_s(u) := 2\frac{RT}{F} \operatorname{asinh}\left(\frac{R_s}{6\varepsilon_s j_0^s A_{\text{cell}} d_s} u\right)$, $\eta_{r,s}(u) := \frac{1}{2A_{\text{cell}}} \left(\frac{d_s}{\sigma_{s,\text{eff}}} + \frac{d_s}{\kappa_s}\right) u$, $\eta_{r,\text{sep}}(u) := \frac{1}{A_{\text{cell}}} \frac{d_{\text{sep}}}{\kappa_{\text{sep}}} u$, $\kappa_s := \kappa_e \varepsilon_{e,s}^{1.5}$, $\sigma_{s,\text{eff}} := \sigma_s \varepsilon_s$, $\kappa_{\text{sep}} := \kappa_e \varepsilon_{e,\text{sep}}^{1.5}$, with R, T, j_0^s, κ_e, $\varepsilon_{e,s}$, $\varepsilon_{e,\text{sep}}$, ε_s and σ_s defined in [12, Table I].

E. State space form

We present the overall state space representation. We introduce for this purpose the state vector $x := (c_{\text{neg},2},...,c_{\text{neg},N_{\text{neg}}},c_{\text{pos},1},...,c_{\text{pos},N_{\text{pos}}}) \in \mathbb{R}^N$ with $N := N_{\text{neg}} - 1 + N_{\text{pos}}$, the input $u = I_{\text{cell}} \in \mathbb{R}$, the output $y = V_{\text{cell}} \in \mathbb{R}$, and $w \in \mathbb{R}^{n_w}$ and $v \in \mathbb{R}^{n_v}$ represent additive exogenous perturbations and measurement noise respectively. We derive the next state space equation

$$\begin{cases} \dot{x} = Ax + Bu + K + Ew \\ y = h_{\text{cor}}(x) + g(u) + v, \end{cases} \tag{8}$$

where the expressions of the matrices $A \in \mathbb{R}^{N\times N}$, $B \in \mathbb{R}^{N\times 1}$ and $K \in \mathbb{R}^{N\times 1}$ are found after [12, (24)]. The function $h_{\text{cor}} : \mathbb{R}^N \to \mathbb{R}$ is defined as, for any $x \in \mathbb{R}^N$, $h_{\text{cor}}(x) := OCV_{\text{pos}}(H_{\text{pos,cor}}x) - OCV_{\text{neg}}(H_{\text{neg,cor}}x + K_1)$, such as $\zeta_{\text{pos,cor}} := H_{\text{pos,cor}}x$ and $\zeta_{\text{neg,cor}} := H_{\text{neg,cor}}x + K_1$, with $H_{s,\text{cor}} \in \mathbb{R}^{1\times N}$ and K_1 are given in [12, (25)].

We are now ready to proceed with the observer design for system (8).

III. State estimation

In this section, we first synthesize an observer for system (8). Then, we correct the estimated concentrations generated by the observer so that they match the concentrations given by the PDEs in (1) asymptotically for constant inputs.

A. Polytopic approach

The proposed observer takes the form

$$\begin{cases} \dot{\hat{x}} = A\hat{x} + Bu + K + L(y - \hat{y}) \\ \hat{y} = h_{\text{cor}}(\hat{x}) + g(u), \end{cases} \tag{9}$$

where $\hat{x} \in \mathbb{R}^N$ is the state vector estimate, $L \in \mathbb{R}^N$ is the observation matrix gain to be designed and $\hat{y}$ is the estimated (corrected) output.

We define the estimation error $e := x - \hat{x}$. The dynamics of the estimation error follows from (8) and (9),

$$\dot{e} = Ae + Ew - L(h_{\text{cor}}(x) - h_{\text{cor}}(\hat{x})) - Lv. \tag{10}$$

We make the next assumption on the OCVs as in e.g., [4], [9], [17].

Assumption 1: For any $s \in \{\text{neg},\text{pos}\}$, there exist constant matrices $C_{s,1}, C_{s,2} \in \mathbb{R}$ such as for any z, $z' \in \mathbb{R}$,

$$OCV_s(z) - OCV_s(z') = C_s(z,z')(z - z'), \tag{11}$$

where $C_s(z,z') := \lambda_1^s(z,z')C_{s,1} + \lambda_2^s(z,z')C_{s,2}$ with $\lambda_i^s(z,z') \in [0,1]$ for $i \in \{1,2\}$ and $\lambda_1^s(z,z') + \lambda_2^s(z,z') = 1$. □

Assumption 1 means that each OCV_s lies in a polytope defined by $C_{s,1}, C_{s,2}$ with $s \in \{\text{neg},\text{pos}\}$. This condition is often verified in practice. Indeed, the OCVs are generally defined on the interval $[0,1]$ and are typically well-approximated by a piecewise continuously differentiable and thus globally Lipschitz function. Then, it suffices to extrapolate the OCVs on $[1,\infty)$ (resp. on $(-\infty,0]$) by using zero order or first order approximations based on the value of the OCVs at 1 (resp. at 0) for Assumption 1 to hold. Then, $C_{s,1}$ and $C_{s,2}$ represent the minimum and maximum slopes of OCV_s, respectively.

Assumption 1 implies that h_{cor}, defined in Section II.E, satisfies the next property.

Lemma 1: Suppose Assumption 1 holds and consider h_{cor} as defined in Section II.E, we have for any $x, x' \in \mathbb{R}^N$

$$h_{\text{cor}}(x) - h_{\text{cor}}(x') = C(x,x')(x - x'), \tag{12}$$

where $C(x,x') := \sum_{i=1}^4 \Lambda_i(x,x')C_i$, with $C_i \in \mathbb{R}^N$ defined in [12, (41)], $\Lambda_i(x,x') \in [0,1]$ for $i \in \{1,2,3,4\}$ and $\sum_{i=1}^4 \Lambda_i(x,x') = 1$. □

Lemma 1 implies that h_{cor} lies in a polytope defined by the vertices C_i with $i \in \{1,2,3,4\}$.

In view of (12), the estimation error dynamics can be written as

$$\dot{e} = (A - LC(x,\hat{x}))e + Ew - Lv. \tag{13}$$

The next theorem provides a sufficient condition to design gain $L \in \mathbb{R}^N$ under which $e = 0$ is globally exponentially stable in absence of noise v and disturbance w, and satisfies $\mathscr{L}_2$-stability properties when the latter are non-zero.

Theorem 2: Suppose Assumption 1 holds and there exist $\varepsilon, \mu_w, \mu_v \in \mathbb{R}_{>0}$, $L \in \mathbb{R}^N$ and $P \in \mathbb{R}^{N\times N}$ symmetric and positive definite such that for any $i \in \{1,...,4\}$

$$\begin{pmatrix} \mathscr{H}_i + \varepsilon I_N & PE & -PL \\ E^\top P & -\mu_w I_{n_w} & 0 \\ -L^\top P & 0 & -\mu_v I_{n_v} \end{pmatrix} \leq 0, \tag{14}$$

with $\mathscr{H}_i := (A - LC_i)^T P + P(A - LC_i)$ then the following hold.

- System (8), (9) is $\mathscr{L}_2$-stable from (w,v) to e with gain less or equal to $\sqrt{\frac{\mu_w}{\varepsilon}}$ and $\sqrt{\frac{\mu_v}{\varepsilon}}$, respectively, in particular, there exist $c \geq 0$ such that for $w, v \in \mathscr{L}_2$, any solution (x,e) to (8), (13) with u a Lebesgue measurable, locally essentially bounded input satisfies $\|e\|_{\mathscr{L}_2,[0,t)} \leq c|e(0)| + \sqrt{\frac{\mu_w}{\varepsilon}}\|w\|_{\mathscr{L}_2,[0,t)} + \sqrt{\frac{\mu_v}{\varepsilon}}\|v\|_{\mathscr{L}_2,[0,t)}$ for any $t \geq 0$.
- $\{(x,e) : e = 0\}$ is uniformly globally exponentially stable when w=0 and v=0, i.e., there exist $\gamma_1 \geq 1, \gamma_2 > 0$ such that for any solution (x,e) to (8), (13) with u a Lebesgue measurable, locally essentially bounded input satisfies $|e(t)| \leq \gamma_1|e(0)|e^{-\gamma_2 t}$ for any $t \geq 0$. □

The matrix inequality in (14) is not linear, however it becomes linear after a standard change of variables, namely $W = PL$. Condition (14) can be easily tested given the model parameters. Also, the order reduction performed in Section II.C appears to be essential for its feasibility. From $\hat{x}$, which represents the concatenation of the estimated concentrations generated by observer (9) $\hat{x} := (\hat{c}_{\text{neg},2},\ldots,\hat{c}_{\text{neg},N_{\text{neg}}},\hat{c}_{\text{pos},1},\ldots,\hat{c}_{\text{pos},N_{\text{pos}}})$, we can retrieve $\hat{c}_{\text{neg},1}$ by replacing the concentrations in (6) by their estimates.

B. Corrected estimated concentrations

Observer (9) generates estimated lithium concentrations, which can also be corrected along with $\hat{c}_{\text{neg},1}$ so that they asymptotically match the concentrations of the PDEs in (1) for constant input currents as seen in Section II.B. We denote in the following $c_{s,(1)}$ the concentrations generated by the PDEs in (1) as in Section II.B and $\hat{c}_s$ the estimated concentrations of electrode s, with $s \in \{\text{pos},\text{neg}\}$.

We denote the corrected estimated concentrations as $\hat{c}_{s,\text{cor}}$, which are given by, for $j \in \{1,\dots,N_s\}$ and $s \in \{\text{neg},\text{pos}\}$,

$$\hat{c}_{\text{s,cor,j}} := \hat{c}_{s,\text{mean}} - K_j^s(\hat{c}_{s,\text{mean}} - \hat{c}_{s,j}), \tag{15}$$

where $\hat{c}_{s,\text{mean}} := \frac{1}{N_s}\sum_{i=1}^{N_s}\hat{c}_{s,i}$ and K_j^s as defined in (3).

The next theorem states an asymptotic property of the error between the corrected estimated concentrations and the concentrations generated by the original PDEs in (1) when time tends to infinity for constant inputs.

Theorem 3: Consider system (8) and its observer (9) and suppose $e = x - \hat{x} = 0$ is globally exponentially stable when $w = 0$ and $v = 0$. Then, for any constant input current I_{cell} and any $c_0 \in \mathbb{R}_{\geq 0}$ such that $c_{s,(1)}(r,0) = c_0$ for all $r \in [0, R_s]$, any corresponding solution $\hat{x}$ to (9) and $c_{s,(1)}$ to (1) satisfy

$$(\hat{c}_{\text{cor}} - c_{(1)})_\infty = 0, \tag{16}$$

where $\hat{c}_{\text{cor}} := (\hat{c}_{\text{neg,cor},1}, \hat{c}_{\text{neg,cor},2}, \dots, \hat{c}_{\text{neg,cor},N_{\text{neg}}}, \hat{c}_{\text{pos,cor},1}, \dots, \hat{c}_{\text{pos,cor},N_{\text{pos}}})$ is the vector of the corrected estimated concentrations and $c_{(1)} := (c_{\text{neg},(1)}(r_1^{\text{neg}},\cdot), c_{\text{neg},(1)}(r_2^{\text{neg}},\cdot), \dots, c_{\text{neg},(1)}(r_{N_{\text{neg}}}^{\text{neg}},\cdot), c_{\text{pos},(1)}(r_1^{\text{pos}},\cdot), \dots, c_{\text{pos},(1)}(r_{N_{\text{pos}}}^{\text{pos}},\cdot))$. □

Theorem 3 implies that, under the conditions of Theorem 2, the estimated corrected lithium concentrations asymptotically match the lithium concentrations of (1) in absence of noise and disturbance provided that a constant input current is applied and $c_{s,(1)}(r,0)$ is uniform for all $r \in [0, R_s]$.

IV. Numerical case study

We simulate model (8) and the model in [5] with the parameters values given in [12, Table I]. We assume that there is no measurement noise and no perturbation. The considered OCVs curves are given in Figure 1, which satisfy Assumption 1. The used input current u is a Plug-in Hybrid Electrical Vehicle (PHEV) discharge current on the time interval $[0, 1800]$, a PHEV charge current on $[1800, 3600]$ and 0 on $[3600, 4500]$, as illustrated in Figure 2. The current profile is thus rapidly varying on [0,3600], during which we will see that improvements are obtained with the corrections presented in Section II.B. We initialize both models at equilibrium, meaning that all the initial concentrations within the same electrode are equal, with a state of charge (SOC) equal to 100%. The SOC is defined by for $s \in \{\text{pos, neg}\}$

$$SOC_s := 100\frac{c_{s,\text{mean}} - c_0^s}{c_{100}^s - c_0^s}, \tag{17}$$

where c_0^s, c_{100}^s are the lithium concentration of electrode s at SOC equal 0% and 100%, respectively. Given that SOC_{pos} and SOC_{neg} are equal, we use the notation SOC instead. As for the reference model, it is obtained by solving the PDEs of (1) using a finite elements method and simulated with the parameters given in [12, Table I], see [18] for details.

We have compared the surface concentrations $c_{s,\text{surf}}$ and the output voltages V_{cell} generated by the model in [5] and model (8), with those generated by the reference infinite-dimensional model over the whole interval of time [0,4500] as well as [0,3600] where the current is rapidly varying in Table I. We have computed the mean absolute error

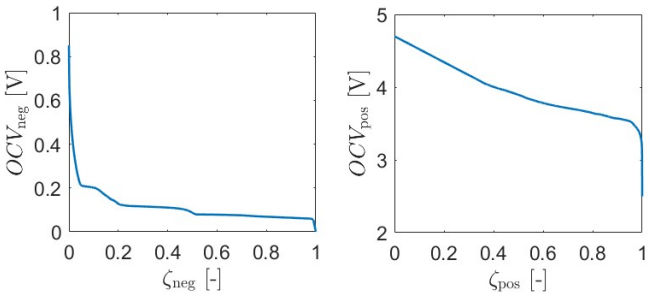

Fig. 1. OCVs curves.

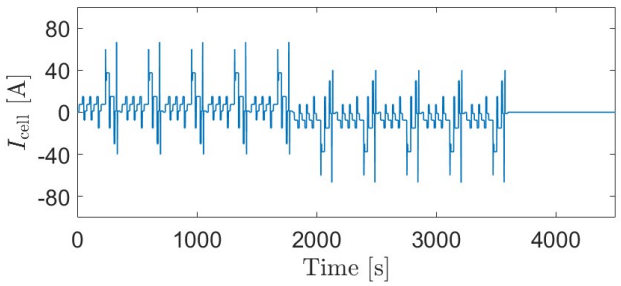

Fig. 2. Input current profile.

(MAE) and the root mean square error (RMSE) of the voltage error $e_{V_{\text{cell}}}$ between V_{cell} generated by (1) and V_{cell} generated by the model in [5] and by (8), respectively and the normalized surface concentrations error $\mathbf{e}_{c_{s,\text{surf}}}$ between the surface concentrations generated by (1) and those generated by the model in [5] and model (8), respectively. We see significant improvement of the output voltage and the surface concentrations given by model (8) compared to the one in [5] on the interval [0,4500] and particularly on [0,3600], when the current is rapidly varying.

	MAE [0,4500]	RMSE [0,4500]	MAE [0,3600]	RMSE [0,3600]
$e_{V_{\text{cell}}}$: model in [5] [mV]	12.1	17.8	14.6	19.8
$e_{V_{\text{cell}}}$: model (8) [mV]	**5.1**	**8.3**	**6.1**	**9.2**
Improvement [%]	**57.85**	**53.37**	**58.22**	**53.54**
$\mathbf{e}_{c_{\text{pos,surf}}}$: model in [5] [%]	2.05	3.01	2.48	3.36
$\mathbf{e}_{c_{\text{pos,surf}}}$: model (8) [%]	**0.95**	**1.53**	**1.15**	**1.71**
Improvement [%]	**53.66**	**49.17**	**53.63**	**49.11**
$\mathbf{e}_{c_{\text{neg,surf}}}$: model in [5] [%]	8.51	11.79	9.93	13.10
$\mathbf{e}_{c_{\text{neg,surf}}}$: model (8) [%]	**5.48**	**7.79**	**6.24**	**8.62**
Improvement [%]	**35.60**	**33.93**	**37.16**	**34.20**

TABLE I

MAE and RMSE of the output voltage and the surface concentrations errors given by model in [5] and model (8).

We have then designed an observer for system (8) and one for the system in [5] by applying the results of Section III.A. We have been able to obtain the same observer gain L in both cases so that the only difference between the two observers is the output equation used to synthesize them. In particular, $L = 10^4$(3.2354,3.5397,3.3862,-5.0338,-5.7366, -5.3258,-5.4284). We have initialized both observers such that all estimated concentrations within the same particle are equal and correspond to a SOC estimate, denoted $\widehat{SOC}$, of 0%. We note that $\widehat{SOC}$ is obtained by replacing $c_{s,\text{mean}}$ in (17) by its estimate $\hat{c}_{s,\text{mean}}$. Both observers are fed by the

voltage output generated by the reference model in [18].

Figure 3 reports the actual SOC given by the infinite-dimensional model and the estimated ones, as well as the corresponding norm of the estimation errors on the SOC $e_{SOC} = SOC - \widehat{SOC}$ obtained with the observer in [4], observer (9) and observer (9) with the correction of its estimated concentrations $\hat{c} := (\hat{c}^{\mathrm{l}}_{\mathrm{neg}}, \hat{x})$ as done in Theorem 3. We see that observer (9) based on the corrected model (8) provides a more accurate SOC. This improvement is quantified by computing the MAE and the RMSE of the SOC estimation errors e_{SOC} for the observer in [4], observer (9) and observer (9) with $\hat{c}_{\mathrm{cor}}$, respectively, averaged over 20 simulations for initial SOC estimates ranging from $\{0\%, 5\%, ..., 100\%\}$. The results are given in Table II. We see that observer (9) generates more accurate results in terms of SOC estimation and this improvement is of the order of percent, which is significant for lithium-ion batteries.

We have also computed in Table II the average MAE and the average RMSE over the same 20 scenarios, of the norm of the normalized estimated concentrations error $\mathbf{e}_{c_s}$ for $s \in \{\mathrm{pos}, \mathrm{neg}\}$ for the observer in [4], for observer (9) and for observer (9) with $\hat{c}_{\mathrm{cor}}$. More accurate estimated concentrations are obtained as a result of the correction of the estimated concentrations.

	MAE	RMSE
e_{SOC}: observer in [4] [%]	1.92	2.76
e_{SOC}: observer (9) [%]	**0.81**	**1.34**
e_{SOC}: observer (9) + $\hat{c}_{\mathrm{cor}}$ [%]	1.59	2.28
$\mathbf{e}_{c_{\mathrm{pos}}}$: observer in [4] [%]	1.16	1.87
$\mathbf{e}_{c_{\mathrm{pos}}}$: observer (9) [%]	1.78	2.35
$\mathbf{e}_{c_{\mathrm{pos}}}$: observer (9) + $\hat{c}_{\mathrm{cor}}$ [%]	**1.02**	**1.64**
$\mathbf{e}_{c_{\mathrm{neg}}}$: observer in [4] [%]	5.82	6.51
$\mathbf{e}_{c_{\mathrm{neg}}}$: observer (9) [%]	7.28	8.19
$\mathbf{e}_{c_{\mathrm{neg}}}$: observer (9) + $\hat{c}_{\mathrm{cor}}$ [%]	**4.99**	**5.58**

TABLE II

AVERAGE MAE AND RMSE OVER 20 SIMULATIONS OF THE SOC ESTIMATION AND OF THE ESTIMATED CONCENTRATIONS ERRORS.

V. CONCLUSION

We have designed an observer based on a finite-dimensional electrochemical model, for which we corrected its lithium concentrations to asymptotically eliminate the errors induced by the PDE discretization for constant currents. Simulations results show the improvement of the model and the state estimates as a result of the proposed corrections.

REFERENCES

[1] J. K. Barillas, J. Li, C. Guenther, and M. A. Danzer. A comparative study and validation of state estimation algorithms for Li-ion batteries in battery management systems. *Applied Energy*, 155:455–462, 2015.

[2] H. Beelen, H. Bergveld, and M. C. F. Donkers. Joint estimation of battery parameters and state of charge using an extended Kalman filter: a single-parameter tuning approach. *IEEE Trans. Control Syst. Technol.*, 29(3):1087–1101, 2021.

[3] M. Benzine, R. Postoyan, S. Raël, S. Benjamin, and D. Monier Reyes. Systematic observer redesign for lithium-ion battery models to account for the electrolyte dynamics. *Submitted for publication*, 2022.

[4] P. Blondel, R. Postoyan, S. Raël, S. Benjamin, and P. Desprez. Observer design for an electrochemical model of lithium-ion batteries based on a polytopic approach. In *IFAC World Congress*, pages 8127–8132, Toulouse, France, 2017.

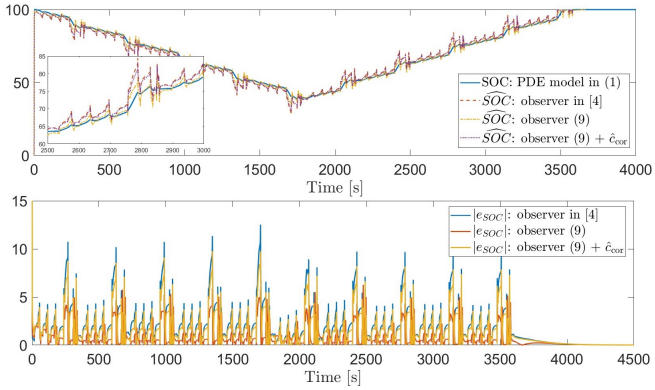

Fig. 3. SOC and $\widehat{SOC}$ generated by the observer in [4], observer (9) and observer (9) with $\hat{c}_{\mathrm{cor}}$ (top) and norm of the estimation errors $e_{SOC} := SOC - \widehat{SOC}$ (bottom).

[5] P. Blondel, R. Postoyan, S. Raël, S. Benjamin, and P. Desprez. Nonlinear circle-criterion observer design for an electrochemical battery model. *IEEE Trans. Control Syst. Technol.*, 27:889–897, 2019.

[6] S. Dey, B. Ayalew, and P. Pisu. Nonlinear robust observers for state-of-charge estimation of lithium-ion cells based on a reduced electrochemical model. *IEEE Trans. Control Syst. Technol.*, 23(5):1935–1942, 2015.

[7] D. Di Domenico, A. G. Stefanopoulou, and G. Fiengo. Lithium-ion battery state of charge and critical surface charge estimation using an electrochemical model-based extended Kalman filter. *ASME J. Dyn. Sys., Meas., Control*, 132(6):1–11, 2010.

[8] M. Doyle, T. F. Fuller, and J. Newman. Modeling of galvanostatic charge and discharge of the lithium/polymer/insertion cell. *J. Electrochem. Soc.*, 140(6):1526, 1993.

[9] H. J. Dreef, H. P. G. J. Beelen, and M. C. F. Donkers. LMI-based robust observer design for battery state-of-charge estimation. In *IEEE Conf. Decis. Control*, pages 5716–5721, Miami Beach, USA, 2018.

[10] T. F. Fuller, M. Doyle, and J. Newman. Simulation and optimization of the dual lithium ion insertion cell. *J. Electrochem. Soc.*, 141(1):1–10, 1994.

[11] H. He, R. Xiong, H. Guo, and S. Li. Comparison study on the battery models used for the energy management of batteries in electric vehicles. *Energy Conv. Manag.*, 64:113–121, 2012.

[12] M. Khalil, R. Postoyan, and S. Raël. Enhancing accuracy of finite-dimensional models for lithium-ion batteries, observer design and experimental validation. *arXiv preprint arXiv:2308.08844*, 2023.

[13] R. Klein, N. A. Chaturvedi, J. Christensen, J. Ahmed, R. Findeisen, and A. Kojic. Electrochemical model based observer design for a lithium-ion battery. *IEEE Trans. Control Syst. Technol.*, 21(2):289–301, 2013.

[14] X. Lin, H. E. Perez, S. Mohan, J. B. Siegel, A. G. Stefanopoulou, Y. Ding, and M. P. Castanier. A lumped-parameter electro-thermal model for cylindrical batteries. *J. Power Sources*, 257:1–11, 2014.

[15] J. Meng, G. Luo, M. Ricco, M. Swierczynski, D.-I. Stroe, and R. Teodorescu. Overview of lithium-ion battery modeling methods for state-of-charge estimation in electrical vehicles. *Applied Sciences*, 8(5):659, 2018.

[16] S. Moura, N. A. Chaturvedi, and M. Krstić. PDE estimation techniques for advanced battery management systems — Part II: SOH identification. In *Amer. Control Conf.*, pages 566–571, Montréal, Canada, 2012.

[17] E. Planté, R. Postoyan, S. Raël, J. Youssef, S. Benjamin, and D. M. Reyes. Multiple active material lithium-ion batteries: Finite-dimensional modeling and constrained state estimation. *IEEE Trans. Control Syst. Technol.*, 31(3):1106–1121, 2023.

[18] S. Raël and M. Hinaje. Using electrical analogy to describe mass and charge transport in lithium-ion batteries. *J. Power Sources*, 222:112–122, 2013.

[19] A. Zemouche, M. Boutayeb, and G. Bara. Observers for a class of Lipschitz systems with extension to H_∞ performance analysis. *Sys. & Control Lett.*, 57:18–27, 2008.